

Variability of feedstock viscosity and its correlation with dimensional variability of green powder injection moulded components

R. Zauner, C. Binet, D. F. Heaney, and J. Piemme

In this study, a correlation between green part dimensional variation and feedstock viscosity variation is presented for the powder injection moulding (PIM) manufacturing process. A correlation of an increase in green part dimensional variation as feedstock viscosity variation increases has been found and the correlation was independent of powder type (316L gas atomised and water atomised) and mixing technique (batch and continuous). The variation of feedstock viscosity was lowest over the greatest temperature range for high shear continuous compounding with a broad distribution of irregularly shaped powder. Thus, this feedstock material would have the greatest process window for injection moulding with the least variation.

PM/1049

Dr Zauner (rudolf.zauner@arcs.ac.at) is with ARC Seibersdorf research GmbH, Materials and Production Engineering, A-2444 Seibersdorf, Austria. Dr Binet, Dr Heaney and Dr Piemme are with the Center for Innovative Sintered Products, Penn State University, 147 Research West, University Park, PA 16802, USA. Manuscript received 20 January 2003; accepted 27 November 2003.

Keywords: Feedstock, Powder injection moulding, Dimensional variability

© 2004 IoM Communications Ltd. Published by Maney for the Institute of Materials, Minerals and Mining.

INTRODUCTION

Powder injection moulding (PIM) has emerged as a viable method of producing complex shaped parts at a competitive cost.¹ The PIM process, which consists of feedstock preparation, injection moulding, debinding and sintering uses a combination of powder metallurgy and plastic injection moulding technologies to produce net shape metal, ceramic or hard materials components.

According to German,² powder injection moulding is an attractive process when the following component features apply: thickness ranging from 0.2 to 20 mm, mass ranging from 0.02 to 1000 g, moderate levels of shape complexity and smooth surfaces. The typical range of tolerances is between 0.1 and 1 mm. German³ gives a guideline as to when to consider PIM as a manufacturing technique. PIM is usually used for

- (i) complex components
- (ii) made of metal, ceramics or other sinterable materials
- (iii) in mass production.

The technology is well established for standard materials (stainless steel, oxide ceramics)¹ and has a market share of almost US\$1bn (2001). In order to increase the window of

application for PIM, the dimensional precision and variability of the manufactured components need to be further understood and improved. Recently, substantial part to part variability has been observed in the green (i.e. injection moulded) state before the components undergo substantial shrinkage during sintering.⁴⁻⁶

The importance of feedstock homogeneity has been pointed out by both part manufacturers and researchers alike, all agreeing that variations induced in the early process stages cannot be eliminated in the subsequent PIM process steps of moulding, debinding and sintering. Therefore, the homogeneity of the feedstock can become a critical characteristic for these later process steps in the PIM process. Inhomogeneities can lead to powder/binder separation, defects (e.g. cracks and voids) or increased distortion and eventually to failure of the PIM manufacturing route.

Supati *et al.*⁷ studied the effects of mixing time, mixing speed, mixing temperature and solids loading on feedstock homogeneity using a torque rheometer. They found that increasing the mixing speed increased mixture homogeneity. The study states that feedstock homogeneity can be predicted by observing the torque values during feedstock compounding; as the torque values plateau, the feedstock becomes homogeneous. The effect of temperature on deagglomeration was also investigated. At excessively high temperatures, the feedstock became inhomogeneous due to powder/binder separation. Their study showed that as the powder loading increased, the maximum torque value increased. They concluded from torque and rheological analysis that higher torque indicates a higher viscosity.

Li *et al.*⁸ investigated rheological properties of multiple binder systems and concluded that good rheological properties are beneficial for dimensional control of PIM components. The rheological properties investigated were viscosity and its dependence on temperature and shear rate, which were used to define a mouldability index. This mouldability index, borrowed from polymer processing, predicts favourable and reproducible moulding for low viscosity, low shear sensitivity and low temperature sensitivity materials. However, these parameters do not always shift favourably dependent upon each other, as predicted, resulting in a complex rheological behaviour.

White and German⁹ studied solids loading and its effect on dimensional variation of 316L injection moulded components. Their main finding was a favourable decrease in dimensional variation as solids loading increased. A tolerance of less than $\pm 0.1\%$ was reported for all sintered dimensions.

Dihoru *et al.*¹⁰ used a combination of capillary and torque rheometry and developed a neural network model to predict the maximum solids loading without powder/binder separation. They found that irregular powder morphology leads to smaller maximum solids loadings but more stable feedstocks in terms of powder/binder separation.

Kulkarni *et al.*¹¹ used the pycnometer density of the feedstock as a homogeneity measure and found it sufficiently sensitive as a tool for quality control in a production environment.

Although multiple studies on the effect of feedstock homogeneity on dimensional stability have been performed, no quantification of the relationship between the variability of viscosity to the variability in green component dimensions has been reported. Therefore, in this work, the influence of the variability of the feedstock viscosity on the green dimensional variability is investigated. High pressure capillary rheometer measurements of both batch and continuously compounded feedstocks were analysed and correlated with green component dimensional variations.

EXPERIMENTAL WORK

Compounding

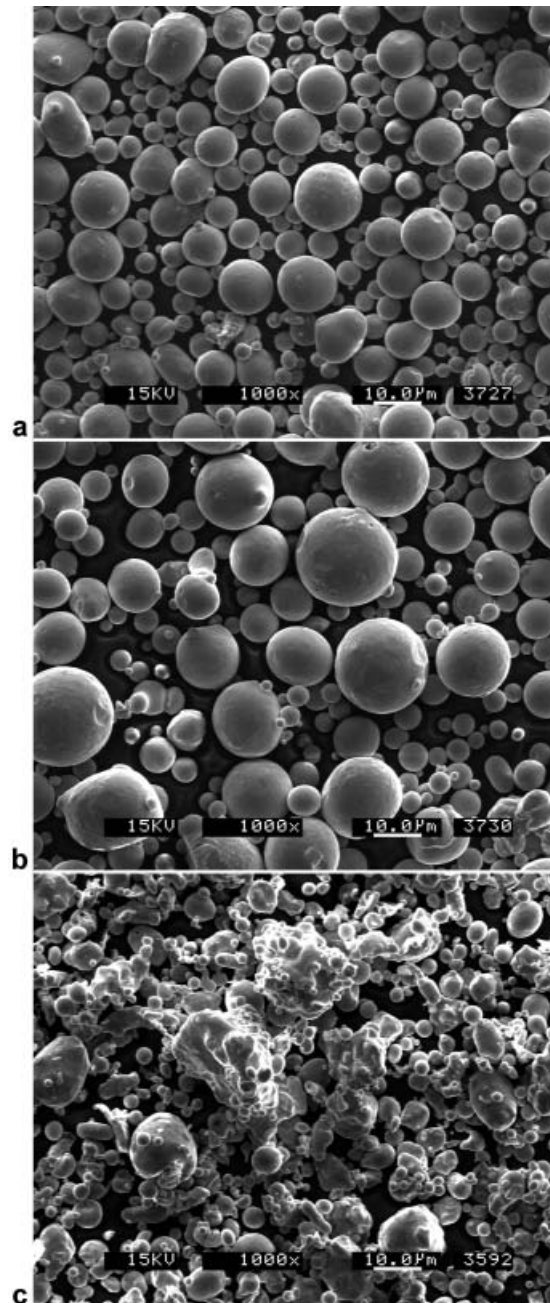
For comparison, three different 316L stainless steel powders were used to prepare different feedstocks. These powders had different particle sizes and shapes, as shown in Fig. 1. Two powders were gas atomised grades, one having a D_{90} of $-16\ \mu\text{m}$ (Fig. 1a) and the other having a D_{90} of $-22\ \mu\text{m}$ (Fig. 1b). The other powder was high pressure water atomised with a D_{90} of $-22\ \mu\text{m}$ (Fig. 1c). Table 1 shows the average of three measurements for the powder characteristics of the different materials. A powder loading of 65 vol.-% was kept as a constant for all feedstocks. The powders were dry mixed with the binder components for 20 min using a turbula powder blender. The binder was a wax-polymer based system and consisted of a wax component, a polymer component, and a polymer based lubricant component.

Compounding of feedstocks can take place in a wide variety of apparatuses. The feedstock can be mixed in either equipment that has a minimal shearing effect on the powder/binder mixture, such as plough shear kneaders, or equipment that involves high and defined shearing, such as corotating twin screw extruders. In order to compare shearing effects, mixing was performed in both a 0.5 L sigma blade batch mixer (Teledyne) at 160°C and a corotating 2 in. twin cam continuous compounder (Readco) at 160°C . Batch mixing was carried out for 30 min, which is in the range of the residence time used for continuous compounding. Continuous compounding was performed twice on the same mixture with granulation between each run. After compounding and cooling, the feedstocks were granulated in an IMS granulator. The specific feedstock properties are listed in Table 2.

Capillary rheometry

The rheological properties of a feedstock are effectively characterised by capillary rheometry measurements. The shear rate range that simulates mould filling lies in a range of $100\ \text{s}^{-1}$ to approximately $100\,000\ \text{s}^{-1}$.¹ A Kayeness Galaxy V capillary rheometer with a tungsten carbide die having an orifice diameter d of 1 mm and a length L of 30 mm resulting in an aspect ratio (L/d) of 30 was used to measure apparent viscosities at different temperatures and shear rates. Viscosity versus shear rate diagrams, produced at different temperatures, were used as a basis for optimising the feedstock properties and selecting proper moulding conditions. Most importantly for this study, it was postulated that the feedstock homogeneity can be determined quantitatively from the time dependent fluctuations of the viscosity at constant shear rates. It is this additional information, which will be analysed and expressed in terms of variability, which will be correlated with green part dimensional variations in the results section.

The homogeneity was measured using the capillary rheometer with a constant ram rate of $100\ \text{mm}\ \text{min}^{-1}$ producing a shear rate of $1180\ \text{s}^{-1}$. Measurements were



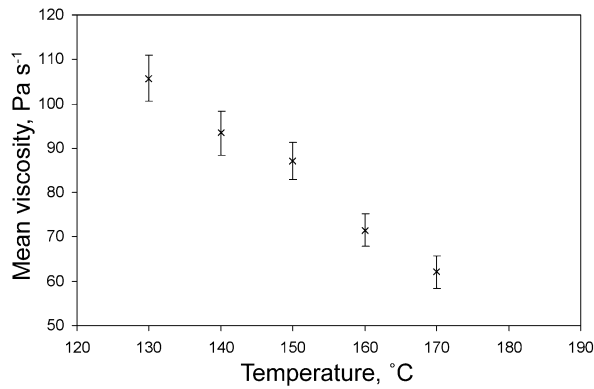
1 SEM micrographs of *a* gas atomised powder, $-16\ \mu\text{m}$; *b* gas atomised powder, $-22\ \mu\text{m}$; *c* water atomised powder, $-22\ \mu\text{m}$

performed at temperatures ranging from 130 to 180°C . The time dependent fluctuations observed in the viscosity measurements are postulated to be a measure of the homogeneity of the feedstock.

Powder injection moulding

From each feedstock 120 components were injection moulded and the green dimensions were measured using a SmartScope, which is an automated measuring system based on an optical microscope coupled with image analysis. From 120 measurements, the variability of the green dimensions was calculated for each feedstock type.

Moulding was performed on a hydraulic 55 ton injection moulding machine using a moulding temperature of 150°C , a mould temperature of 35°C , an injection speed of $20\ \text{cm}^3\ \text{s}^{-1}$, and a hold pressure of 25 MPa cavity pressure with cavity pressure controlled switch over.

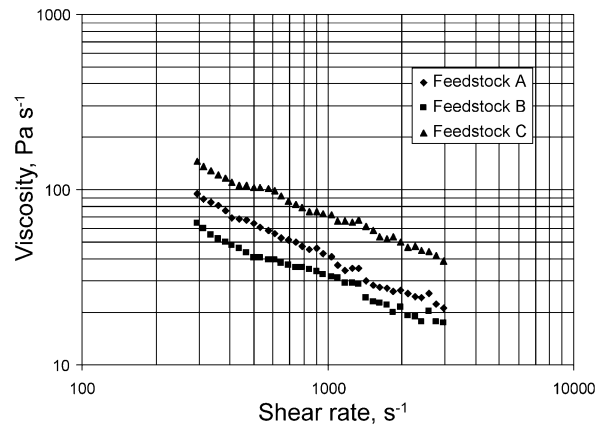


2 Temperature dependence of viscosity for feedstock C (water atomised, 65% solids loading)

RESULTS

Viscosity dependence on temperature

Figure 2 shows a typical viscosity versus temperature plot for feedstock C where the Arrhenius type dependence of viscosity on temperature becomes apparent. The error bars show the fluctuations in the measurement in terms of the variability in viscosity. The three different powder types used in this study are very different in particle shape, size and/or surface area; therefore, the viscosity of the different compounds produced using these different powders at the same temperature is also different. Table 3 summarises these results. The irregular water atomised powder particles of feedstocks C and D do not flow as easily under shear stress as their gas atomised counterparts of feedstocks A and B, thus, resulting in greater overall viscosity. The viscosity of feedstock A is higher than that of the feedstock B since the smaller powder used in feedstock A has a



3 Viscosity dependence on shear rate for different feedstocks at 160 °C

higher resistance against flow than the larger powder used in feedstock B. The higher surface area powder requires more binder for powder wetting and leaves less binder for flow modification. At low temperatures, a deviation from the expected Arrhenius behaviour was observed for feedstocks A and B.

Viscosity dependence on shear rate

All four feedstocks showed the typical shear rate thinning effect known for polymers: with increasing shear rate, the viscosity decreased. Figure 3 shows the viscosities and that the shear rate effect is strongest for feedstock A, as is evident by its increase in negative slope when compared with feedstocks B and C. Feedstocks B and C show very similar shear rate dependence. This observation could be

Table 1 Powder properties

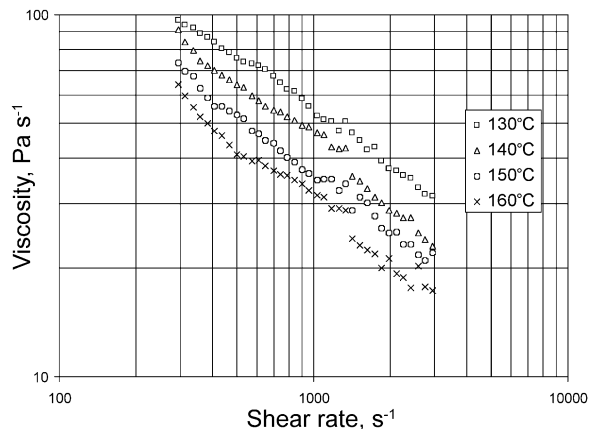
	Particle size, μm			Densities, g cm^{-3}			Surface area, $\text{m}^2 \text{g}$
	D_{10}	D_{50}	D_{90}	Apparent	Tap	Pycnometer	5-point BET
Gas atomised, $-16 \mu\text{m}$	5.93	10.56	16.31	4.13	4.88	7.90	0.126
Gas atomised, -22μ	6.05	12.80	21.38	4.05	4.95	7.92	0.119
Water atomised, $-22 \mu\text{m}$	4.01	10.98	23.05	3.04	4.00	7.85	0.247

Table 2 Feedstock nomenclature

Feedstock	Powder type	Compounding technique
A	Gas atomised, $-16 \mu\text{m}$	Corotating twin cam compounder
B	Gas atomised, $-22 \mu\text{m}$	Corotating twin cam compounder
C	Water atomised, $-22 \mu\text{m}$	Corotating twin cam compounder
D	Water atomised, $-22 \mu\text{m}$	Sigma blade batch mixer

Table 3 Mean and variability of viscosity at 1180 s^{-1}

Feedstock	Temperature, $^{\circ}\text{C}$	Viscosity, Pa s^{-1}	Variability	Feedstock	Temperature, $^{\circ}\text{C}$	Viscosity, Pa s^{-1}	Variability
A	130	56.0	0.091	C	130	105.7	0.049
	140	46.9	0.070		140	93.4	0.054
	150	47.6	0.042		150	87.1	0.049
	160	47.1	0.035		160	71.5	0.051
	170	37.5	0.070		170	62.1	0.060
B	130	44.2	0.046	D	130	125.0	0.104
	140	47.5	0.060		150	142.8	0.072
	150	50.0	0.091		160	126.7	0.057
	160	47.0	0.132		170	91.8	0.052
	170	42.1	0.167		180	73.0	0.089



4 Temperature dependence of viscosity for feedstock B

related to the $-16\ \mu\text{m}$ gas atomised powder of feedstock A having the smallest mean particle size and narrowest particle size distribution. This finding however needs to be addressed in a more detailed study.

The dependence of the viscosity on the shear rate at different temperatures is shown for feedstock B in Fig. 4. The temperature range is fairly limited: the upper limit is controlled by the starting decomposition of the wax component, and the melting temperature of the polymer binder component controls the lower temperature limit. According to TGA-DTA data, the melting point of the highest melting component of the binder system is around 130°C .

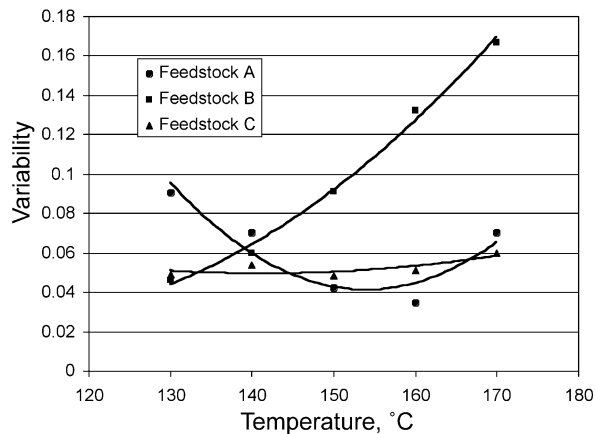
Variability of viscosity

Applying a constant shear rate and monitoring the fluctuations over time was the basis for quantifying the variability of the feedstock viscosity. The fluctuations were expressed as a standard deviation from the mean and provided a quantitative measure of the homogeneity: the higher the homogeneity of a feedstock, the smaller its fluctuations and the smaller the standard deviation. The intrinsic variability of the capillary rheometer was measured with the binder components without powder and found to be in the range of 0.9 to 3.5% of the variability of the feedstock viscosity (measured with powder) at various temperatures. The feedstocks were tested at different temperatures and the variability, which is calculated from the standard deviation normalised by the mean. Five runs were performed for each condition, with each measurement cycle per run lasting 60 s. The results are summarised in Table 3 and shown in Figs. 5 and 6, where the variability is plotted for the different feedstocks as a function of the temperature.

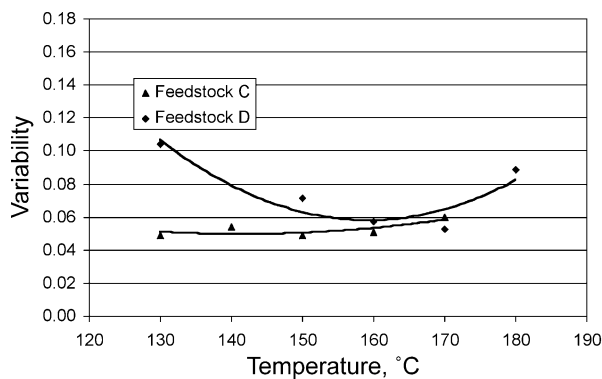
Feedstock B (gas atomised, $-22\ \mu\text{m}$) shows an increase in variability with increasing temperature (Fig. 5). At 170°C the variability is around four times as high as that at 130°C . At temperatures above 150°C , feedstock B had the highest variability in viscosity of all the feedstocks investigated.

In contrast, feedstock A (gas atomised, $-16\ \mu\text{m}$) exhibited minimal variability between 150 and 160°C (Fig. 5). In this temperature range the variability dropped and significantly increased at higher and lower temperatures. The optimum processing window to reduce variability for injection moulding feedstock A is predicted to be between 150 and 160°C .

The variability of feedstock C (water atomised) showed the smallest sensitivity to temperature, with insignificant variations within the range of temperatures tested (Figs. 5 and 6). This is hypothesised to be related to the broader particle size distribution of feedstock C, which has an



5 Temperature dependence of viscosity variability for feedstocks A, B and C



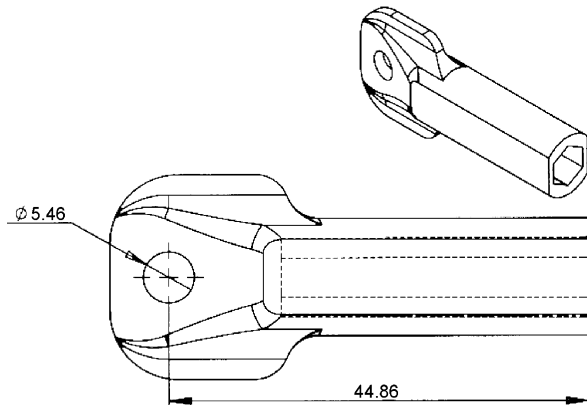
6 Temperature dependence of viscosity variability for feedstocks C and D

equalising effect on the flow behaviour. Similar results were found by Dihoru *et al.*¹⁰ who state that an irregular powder morphology leads to more stable feedstocks in terms of powder/binder separation.

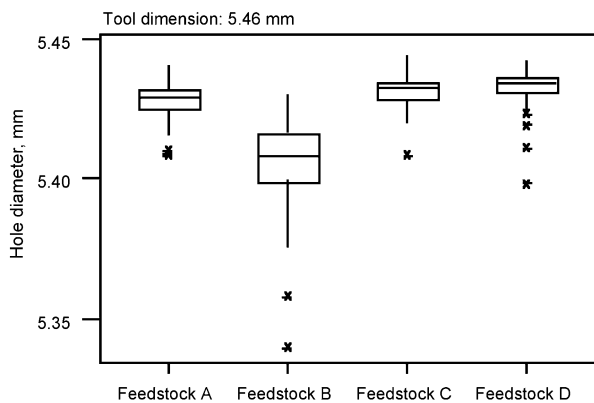
Figure 6 depicts a comparison between continuously compounded and batch compounded feedstocks. The temperature dependence of the variability of batch compounded feedstock D is far higher than that of continuously compounded feedstock C, which was described earlier. This could be an indication that the irregular powder has not been fully wetted by the binder components and therefore only performs well when sheared in an optimum temperature range. Under ideal temperature conditions (160 to 170°C), however, its variability was found to be just as good as that of continuously compounded material.

Variability of green components

Figure 7 shows a drawing of the PIM component used to study green dimensional variability. The dimension study was performed on a core hole diameter (tool dimension $5.46\ \text{mm}$). Figure 8 shows, as an example, the green dimensional variation in the core hole dimension of the green component for feedstocks A, B, C and D. The graph was plotted using Minitab software and shows a line drawn across the box at the median, the bottom of the box at the first quartile (Q1) value and the top at the third quartile (Q3) value. The whiskers extend from the top and bottom of the box to the adjacent values, which are the lowest and highest observations that are still inside the region defined by the following limits: a lower limit of $(Q1 - 1.5(Q3 - Q1))$ and an upper limit of $(Q3 + 1.5(Q3 - Q1))$. Outliers are points outside of the lower and upper limits and are plotted



7 Geometry of PIM component



8 Dimensional variability of component hole

with asterisks (*); outliers were most likely caused by flash, which in turn caused erroneous measurements.

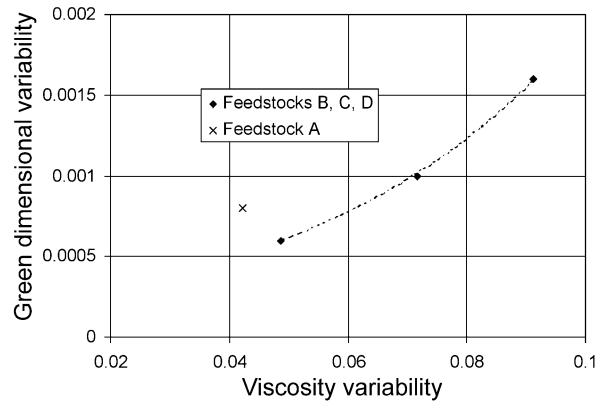
When comparing the green dimensions to the tool dimensions, the experiments showed shrinkage of the green component hole ranging from 0.50% (feedstock C) to 0.35% (feedstock B). This is to be expected since polymer injection moulding typically accounts for a 0.2 to 1% shrinkage.

The dimensional variation in the green state showed a clear dependence on both powder size and type. The variation was largest for feedstock B and smallest for feedstock C. These results were consistent for all other green dimensions of the component geometry.

Viscosity variability versus green dimensional variability

To date, the dimensional variation observed in green PIM components has not been explained.⁴⁻⁶ However, this study's correlation between feedstock viscosity variability and green dimensional variability of the components provides an explanation.

At a moulding temperature of 150°C, the variabilities of the viscosities measured and the green dimensions can be compared. Feedstock B, which had the highest variability in viscosity, caused the highest variability in green part dimensions. Feedstocks A and C, which both showed a far smaller variability in viscosity, gave far less green dimension variation. Comparing the batch and continuously compounded feedstocks C and D, the batch compounded material D shows a slightly higher variability in viscosity, which is reflected in a slightly higher green dimensional variability. A semiquantitative correlation of higher dimensional variability as viscosity variability increases can be extracted from Fig. 9. The data correlated very well when



9 Green dimensional variability versus variability of viscosity at 150°C (moulding temperature)

analysed separately for different particle sizes (-22 µm: feedstocks B, C and D; -16 µm: feedstock A). The small number of data points does not permit quantitative interpreting the results. Qualitatively, however, the viscosity fluctuations measured using a capillary rheometer correlate very well with dimensional variations of the green components, even if the powder shape, particle size distribution and compounding technique are different. For feedstock A, which was compounded with a finer (-16 µm) and narrower powder size distribution powder, a higher variability in the green dimensions was observed than for the coarser powders. These findings are of fundamental importance for the capability of the PIM process; in order to minimise the dimensional variability in later stages of the process, the temperature dependence of the feedstock viscosity fluctuations can be studied and the process parameters, for example the temperature profile in the injection moulding machine, selected on the basis of these findings. For feedstocks B and C, for example, the chosen moulding temperature of 150°C was close to the optimum, while for feedstock A, a lower temperature might have been advantageous in order to avoid the far larger green dimensional variations observed.

CONCLUSIONS

The variations found in the viscosity of a feedstock can be correlated with variations in the dimensions of injection moulded components. Thus, capillary rheometry can be an important tool for predicting the dimensional variability of green powder injection moulded components. The correlation between the viscosity and green part variability could be applied to different powder types, shapes and particle size distributions and for different feedstock compounding techniques, i.e. continuous and batch compounding.

Using the viscosity data, an optimum temperature range for the temperature profile during injection moulding can be determined which helps to minimise green dimensional variations. For different powder types and the same binder system and solids loading, the optimum temperature range differed. In addition, the sensitivity of the variability to temperature was very different from powder to powder and depended on the compounding method used.

ACKNOWLEDGEMENTS

This project was financed in part by a grant from the Commonwealth of Pennsylvania, Department of Community and Economic Development (PTIA #21-116-0011).

REFERENCES

1. R. M. GERMAN and A. BOSE: 'Injection molding of metals and ceramics'; 1997, Princeton, NJ, MPIF.
2. R. M. GERMAN: 'Advances in powder metallurgy and particulate materials', Vol. 5, 71–83; 1998, Princeton, NJ, MPIF.
3. R. M. GERMAN: *Inject. Mold. Mag.*, 2002, **10**, 82–84.
4. T. J. WEAVER, K. F. HENS and R. M. GERMAN: 'Advances in powder metallurgy and particulate materials', Vol. 6, 71–78; 1995, Princeton, NJ, MPIF.
5. R. ZAUNER, D. HEANEY, J. PIEMME, C. BINET and R. M. GERMAN: 'Advances in powder metallurgy and particulate materials'; 2002, Princeton, NJ, MPIF.
6. R. ZAUNER, D. HEANEY, J. PIEMME, C. BINET and R. M. GERMAN: 'Advances in powder metallurgy and particulate materials'; 2002, Princeton, NJ, MPIF.
7. R. SUPATI, N. H. LOH, K. A. KHOR and S. B. TOR: *Mater. Lett.*, 2000, **46**, 109–114.
8. Y. LI, B. HUANG and X. QU: *Powder Metall.*, 1999, **42**, 86–90.
9. G. R. WHITE and R. M. GERMAN: 'Advances in powder metallurgy and particulate materials', 121–132; 1993, Princeton, NJ, MPIF.
10. L. V. DIHORA, L. N. SMITH, R. ORBAN and R. M. GERMAN: *Mater. Manuf. Process.*, 2000, **15**, 419–438.
11. K. M. KULKARNI and W. R. MOSSNER: *PM Sci. Technol. Briefs*, 1999, **1**, 23–26.